Breast Blood Perfusion (BBP) Model and Its Application in Differentiation of Malignant and Benign Breast

Sourav Pramanik[1(✉)], Debapriya Banik[1], Debotosh Bhattacharjee[1], Mita Nasipuri[1], and Mrinal Kanti Bhowmik[2]

[1] Department of Computer Science and Engineering, Jadavpur University, Kolkata, India
{srv.pramanik03327, debu.cse88}@gmail.com, {debotosh, mnasipuri}@cse.jdvu.ac.in
[2] Department of Computer Science and Engineering, Tripura University (A Central University), Agartala, Tripura, India
mrinalkantibhowmik@tripurauniv.in

1 Introduction

Nowadays, medical infrared breast thermography has emerged as an essential tool for early detection, better diagnosis, and effective treatment of breast cancer [1]. It generally records the variation of temperature on the breast surface using IR radiation discharged from the breast surface [3]. Some researches on breast cancer reveal that the abnormal growth rate of a tumor is proportional to its temperature [2]. The changes in thermal patterns occur due to various causes such as inflammation, the presence of a tumor, or angiogenesis. The thermal infrared camera can record these changes very well and thus, breast thermal image can be used to detect breast abnormality in its early stage [4]. However, from the perception of thermal characteristics, it has been seen that a higher level of blood perfusion from any source of abnormality causes heat to be conveyed from the core of the breast to the breast surface with a much greater efficiency. These underlying facts motivated us to derive a breast blood perfusion (BBP) image model from the original gray-level breast thermogram. However, it is very hard to find any related work that uses BBP image for the identification of the breast abnormalities. Over the past few decades, a lot of works have been reported in the literature for the identification of breast abnormalities by directly using the originally captured breast thermograms [5–9]. But unfortunately, they have not achieved any acceptable accuracy so far. Pramanik et al. [5] have proposed a new block variance measure to convert grayscale thermal breast image (TBI) into the corresponding texture features image to predict breast abnormality. Gaber et al. [6] have extracted 30 features from each breast of an individual to detect an abnormality in the breast. Sathish et al. [7] have extracted first- and second-order statistical features by computing histogram and GLCM matrices in four directions. Krawczyk et al. [8] performed asymmetry analysis by taking a set of 38 statistical features from each breast. Gogoi et al. [9] have extracted a total number of six first-order statistical features for asymmetry analysis to differentiate between healthy and unhealthy breasts.

S. Bhattacharyya et al. (eds.), *Advanced Computational and Communication Paradigms*, Lecture Notes in Electrical Engineering 475,
https://doi.org/10.1007/978-981-10-8240-5_45

However, in contrast to the TBI processing, blood perfusion information has widely been used in the thermal face recognition [10]. They have shown that the blood perfusion information is more powerful and consistent than the raw thermograms for the identification of the face. Therefore, in this work, we have proposed a blood perfusion image model, called BBP model, based on an existing model [10] to convert the raw breast thermogram into the blood perfusion image. The fundamental difference between the proposed BBP model and the existing model [10] is that the BBP model has paid a special attention to the pathological condition, which is ignored in [10]. After transformation of the raw breast thermogram into the BBP image, a new combination of texture features is extracted for the analysis of the breast thermograms and fed to the feed-forward artificial neural network (FANN) for classification. Our experimental evaluation on a dataset of benign and malignant breast thermograms outperforms in terms of classification accuracy, sensitivity, specificity, PPV, and NPV compared to the raw gray-level TBI and existing blood perfusion image model [10].

The rest of the paper is arranged as follows. Section 2 demonstrates the proposed system in detail. Section 3 describes the experiment conducted along with performance analysis of the proposed system, and the conclusion is drawn in Sect. 4.

2 Proposed System

Figure 1 shows the flow diagram of the proposed breast abnormality prediction system using TBI. Each of the steps in Fig. 1 will be described in the following subsections.

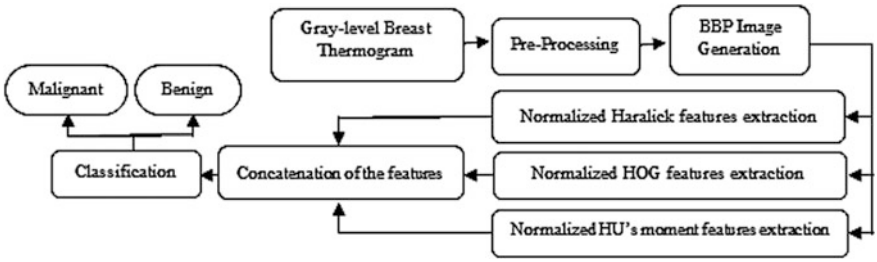

Fig. 1. Flow diagram of the proposed system

2.1 Preprocessing

Usually, in the original thermograms, some extra body parts (arms, neck, and abdomen) also appear beside the breast region as shown in Fig. 2a. Due to the difficulties in the automatic segmentation of the breast region, we have manually segmented the breast region into left and right breast by taking expert's suggestions, as shown in Fig. 2b.

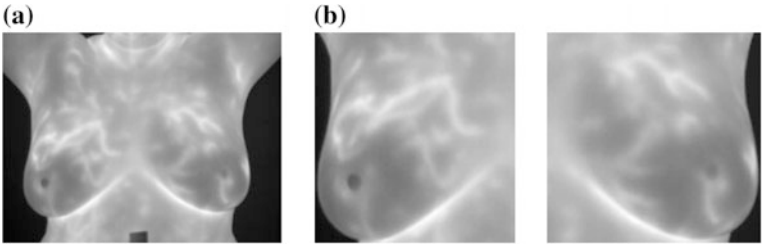

Fig. 2. **a** Original breast thermogram **b** Manually segmented left and right breast region

2.2 Breast Blood Perfusion (BBP) Image Generation

The breast thermogram usually indicates the surface temperature of the breast. The active rise in the temperature of the breast surface is due to the transport of blood through the veins, which are superficial to the skin surface. Hence, the venous patterns on the skin surface play a crucial role in the assessment of the physiological state of the breast thermograms. In this work, we thus converted the breast thermogram into the BBP image to further analyze it.

Wu et al. [10] have proposed a skin heat transfer (SHT) model, which is also called the blood perfusion image model to convert thermal face images into the corresponding blood perfusion face images. This model has made the following assumptions: (1) the body temperature is supposed to be constant with no thermal regulation, (2) the surrounding temperature is generally assumed to be lower than the body temperature, and (3) psychological and pathological conditions are ignored. However, the SHT model has some useful properties (proof is given in [10]) that motivated us to use it in our work. The properties are it preserves the exact shape and location of the objects; it increases the contrast on the high-temperature area and decreases the contrast on the low-temperature area. Although it works well for the face images, we cannot directly apply it to the TBIs because the capturing conditions and pathological conditions of the breast are completely different from the face. Thus, we have modified the SHT model for the application to the TBI.

In a thermally neutral condition, heat equilibrium equations can be defined at the skin surface [11]:

$$T_r + T_e + T_f = T_c + T_m + T_b, \tag{1}$$

where T_c, T_m, *and* T_b are the body heat production elements and stand for deep body conduction, metabolic heat, and blood flow convected heat, respectively. T_r, T_e, and T_f are the outflows terms and stands for radiation, basic evaporation, and convection, respectively.

In Wu et al. [10] model, they have ignored evaporative heat loss T_e because under the equilibrium state evaporative heat loss is very low. Similarly, the metabolic heat component T_m is considered as a constant term in the SHT model (Assumption 3). In our work, TBIs are used to identify the presence of abnormality in the breast. Hence, metabolic heat cannot be a constant term. Based on the above argument, we have proposed a new SHT model, called BBP model, which incorporated the SHT model

along with a new metabolic heat term. Theoretical justification of the proposed BBP model is similar to the SHT model [10]. The following parameters T_r, T_f, T_c, and T_b in (1) are directly obtained from the SHT model and depicted in (2), (3), (4), and (5). T_m is the metabolic heat defined in (6) [11].

$$T_r = \varepsilon\sigma\left(t^4 - t_e^4\right) \tag{2}$$

$$T_f = Ak_f d^{3M-1}\left(P_r g\beta/\nu^2\right)^M (t - t_e)^{M+1} \tag{3}$$

$$T_c = \frac{k_s(t_c - t)}{D} \tag{4}$$

$$T_b = \alpha c_b \omega_b (t_a - t) \tag{5}$$

$$T_m = m_0 * 2^{(t-t_a)/10} \tag{6}$$

where t is the apparent temperature of the skin, t_e is the environmental temperature, $\varepsilon = 0.98$ is the emissivity of the body, σ is the Stefan–Boltzmann constant, A and M are constants, d is the length of the object, P_r is the Prandtl number, g is the local gravitational acceleration, β is the air thermal expansion coefficient, v is the kinematic viscosity of air, k_f is the air thermal conductivity, k_s is the skin thermal conductivity, t_c is the core body temperature, D signifies the distance from the skin to the body core, α is the skin countercurrent exchange ratio, c_b signifies the specific heat of the blood, ω_b is the blood perfusion rate, t_a is the arterial or core body temperature, and m_0 is the metabolic constant, respectively.

From the above equations, it can be seen that there are various controlling parameters associated with the equations. The appropriate estimation of these parameters plays a vital role during the transformation. Thus, by several trial and errors, we have selected the value of the parameter, which is best suited for our domain of application. Table 1 depicts the parameters' values used for our case. Finally, based on the above equations, the BBP model can be obtained as follows:

Table 1. Parameters and their values used in Eq. (7)

Parameter	Value	Parameter	Value
σ	$5.67 * 10^{-8}$ W/m^{2}k^4	β	3.354×10^{-3} K^{-1}
t_e	292.15 K	v	1.56×10^{-5} m^2/s
A	0.29	k_s	0.5 W/mK
M	0.25	t_c	310.15 K
k_f	0.024 W/mK	α	0.8
d	0.170	ρ_b	1060 kg/m^3
D	0.085	c_b	0.92 cal/ml.K
P_r	0.72	t_a	310.15 K
g	9.8 m^2/s	m_0	0.0144

$$I^{(BP)} = \omega_b \frac{\varepsilon\sigma\left(t^4 - t_e^4\right) + Ak_f d^{3M-1}\left(\frac{P_r g\beta}{\nu^2}\right)^M (t - t_e)^{M+1} - \frac{k_s(t_c - t)}{D} - m_0 * 2^{(t-t_a)/10}}{\alpha c_b(t_a - t)} \quad (7)$$

From the perspective of breast thermography, it can be easily visually demonstrated by naked eye that the BBP image enhances the contrast of the high-temperature region and suppresses the contrast of the low-temperature region. As a result, the pathological variations can be easily diagnosed. Figure 3a shows the gray-level left and right breast thermogram, whereas Fig. 3b demonstrates the left and right BBP image.

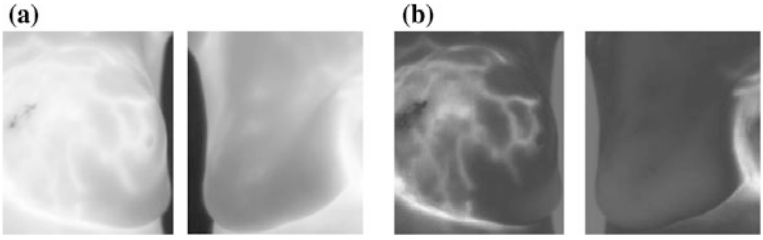

Fig. 3. **a** Gray-level breast thermograms **b** Corresponding BBP images

2.3 Feature Extraction

After transformation of the TBIs into the blood perfusion images, the following three types of features are extracted: texture features (Haralick features), gradient-based features (HOG features), and Hu's moment invariants.

The basis of Haralick texture features is the gray-level co-occurrence matrix (GLCM) [12]. Basically, computation of Haralick features involves two steps. The GLCM is computed in the first step, which describes the texture of the image followed by the extraction of texture features from the GLCM. A set of 14 Haralick texture features are extracted from the co-occurrence matrix. The feature sets are then normalized using z-score [13]. Histogram of oriented gradients (HOG) captures local edge or gradient structure from an image [14]. It is significant for breast thermograms with weak or blur edges and independent of local edge orientation. In this study, HOG is computed by dividing the image into smaller nine rectangular blocks, which are followed by nine bins histogram generation per block. The nine histograms with nine bins were concatenated to form an 81-dimensional feature vector. The gradients were locally normalized over each cell. Hu's moment invariants are computed based on the information provided by both the shape boundary and its interior region. The features extracted from Hu's moment are invariant to rotation, scaling, and translation and so the breast thermograms are independent of any geometric transformation [15]. In this work, a set of seven normalized Hu's moment invariants are calculated based on the central moments, which are invariant to image translation.

Each of the normalized feature sets is then concatenated to form 102-elements feature vector for each of the left and right breasts. Finally, the asymmetry features are calculated for each patient's breast thermogram by taking the absolute difference

between $\left[f_v^{(L)}\right]_{1\times102}$ and $\left[f_v^{(R)}\right]_{1\times102}$, where these are concatenated feature vectors of left and right breast thermogram of each patient. Let $[F]_{1\times102}$ be the asymmetry feature vector of a patient's breast thermogram and is defined as $F = \left|f_v^{(L)} - f_v^{(R)}\right|$.

3 Experimental Results

The breast thermograms used in this research work are collected from the existing Database for Mastology Research (DMR) database [16]. DMR is an available online database that includes 287 breast thermograms of normal, benign, and malignant patients. From the dataset, we have randomly chosen 150 frontal view TBIs (45 malignant and 105 benign) to validate the proposed system.

Here, we have shown the effectiveness of our proposed BBP image for the differentiation of the malignant patients from the benign patients. The 102-elements feature vector is formed for each patient's breast thermogram, which is then fed to the three-layer FANN for the classification [5]. 102 neurons in the input layer of the network are considered to fit the 102-elements feature vector. Since our problem of classification is a binary problem; we have considered one neuron in the output layer. One hidden layer with 51 neurons is considered for this network. For the training of the network, the Levenberg–Marquardt backpropagation algorithm (with learning rate = 0.1) is used. 75 (35 malignant and 40 benign) BBP images are randomly chosen from a set of 150 BBP images (45 malignant and 105 benign) to train the network. Remaining TBIs are used to test the network. We have performed some classical performance measurements such as accuracy, sensitivity, specificity, NPV, and PPV based on the classification results [4]. In this work, the obtained accuracy, sensitivity, specificity, NPV, and PPV are 98%, 93.5%, 100%, 97.1%, and 100%, respectively. In order to verify the superiority of the proposed BBP image over the existing blood perfusion image (EBPI) model [10] and raw grayscale image (RGI), the same set of features are extracted and fed to the FANN classifier. Table 2 shows the experimental results for three types of TBIs. From Table 2, it can be seen that the proposed BBP image-based breast abnormality prediction system achieved significantly better results compared to other two different image-based methods.

Table 2. Comparison of performance measures

Methods	Accuracy (%)	Sensitivity (%)	Specificity (%)	PPV (%)	NPV (%)	AUC
RGI-based method	89	70.9	97.1	91.6	88.1	0.929
EBPI-based method [10]	91	77.4	97.1	92.3	90.5	0.941
Proposed method	**98**	**93.5**	**100**	**100**	**97.1**	**0.976**

We have also quantified our classification results using receiver operating characteristic (ROC) curve. The area under the curve (AUC) is very much informative for the analysis of the system results, which typically lies between 0.5 and 1 [17]. Figure 4 shows the comparison between the ROC curves of the proposed BBP image-based method, raw grayscale image-based method, and existing BPI-based method. The obtained AUC value for our proposed model is 0.976 and attained 100% true positive recognition at a value less than 0.1 false positive rate.

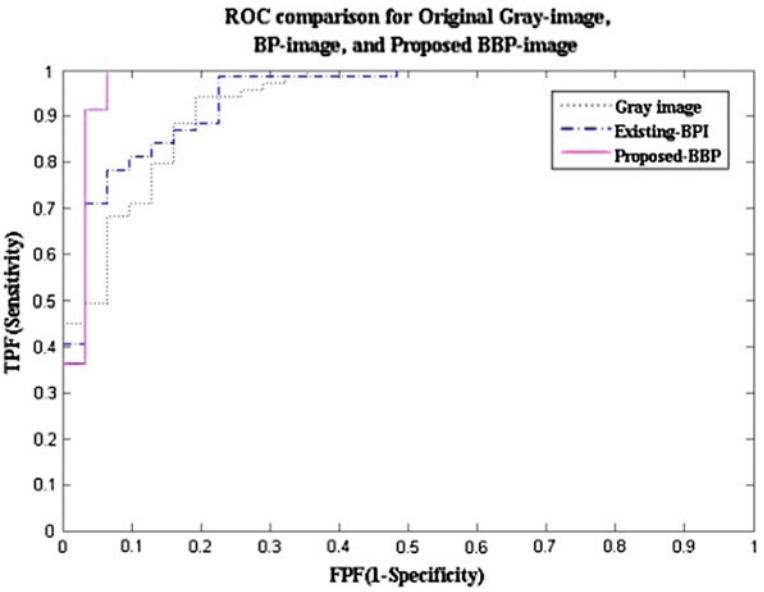

Fig. 4. Comparison of the ROC curves

4 Conclusion

Preprocessing of the TBI plays a crucial role in the computer-assisted diagnosis of breast cancer using TBIs. The raw breast thermogram often suffers from the intra-class scatter problem that makes it very difficult to differentiate a malignant breast thermogram from the benign one. Hence, in this paper, we have proposed a BBP model, which is also the primary contribution of this paper, to convert the raw gray-level breast thermogram into the blood perfusion image. The BBP model used thermal physiology of the breast and reduced the intra-class variability of the breast thermograms. The BBP model can be used as a preprocessing step for the diagnosis of the breast using breast thermogram. The experiment results have shown that the blood perfusion image of the breast is more powerful than the raw gray-level breast thermogram for the prediction of the breast abnormalities. Additionally, we have introduced a new combination of texture features for the analysis of the breast thermograms. In future, we will try to address the problem of suspicious region segmentation using BBP image, which is comparatively very hard for the gray-level breast thermal image.

Acknowledgements. Authors are thankful to DBT, Govt. of India for funding a project with Grant no. BT/533/NE/TBP/2014. Sourav Pramanik is also thankful to Department of Electronics and Information Technology (DeitY), Government of India, for providing him PhD Fellowship under Visvesvaraya PhD Scheme.

References

1. Prabha S, Anandh KR, Sujatha C M, Ramakrishnan S (2014) Total variation based edge enhancement for level set segmentation and asymmetry analysis in breast thermograms. IEEE Int Conf Eng. Med Biol Soc
2. Usuki H, Onoda Y, Kawasaki S, Misumi T, Murakami M, Komatsubara S, Teramoto S (1900) Relationship between thermographic observations of breast tumors and the DNA indices obtained by flow cytometry. Biomed Thermol 10(4):282–285
3. Sobti P, Sobti L, Keith G (2005) Screening and diagnostic mammography: why the gold standard does not shine more brightly? Int J Fert Women Med 50:199–206
4. Borchartt TB, Conci A, Lima RCF, Resmini R, Sanchez A (2013) Breast thermography from an image processing viewpoint: a survey. Sig Proc 93:2785–2803
5. Pramanik S, Bhattacharjee D, Nasipuri M (2016) Texture analysis of breast thermogram for differentiation of malignant and benign breast. IEEE Int Conf Advanc Comput Commun Informat
6. Gaber T, Ismail G, Anter A, Soliman M, Ali M, Semary N, Hassanien AE, Snasel V (2015) Thermogram breast cancer prediction approach based on Neutrosophic sets and fuzzy c-means algorithm. IEEE Int Conf Eng Med Bio Soc
7. Sathish D, Surekha K, Keerthana P, Rajagopal K, Roshan JM (2016) Asymmetry analysis of breast thermograms using automated segmentation and texture features. J Signal Imag Video Process 1–8
8. Krawczyk B, Gerald S (2014) A hybrid classifier committee for analysing asymmetry features in breast thermograms. J Appl Soft Comput 112–118
9. Gogoi US, Majumdar G, Bhowmik MK, Ghosh AK, Bhattacharjee D (2015) Breast abnormality detection through statistical features analysis using infrared thermograms. IEEE Int Sympos Advanc Comput Commun 258–265
10. Wu S, Lin W, Xie S (2008) Skin heat transfer model of facial thermograms and its application in face recognition. Patt Recogn 41:2718–2729
11. Houdas Y, Ring EFJ (1982) Human body temperature: its measurement and regulation. Plenum Press, New York
12. Haralick RM (1979) Statistical and structural approaches to texture. Proc IEEE 67:786–804
13. Jain A, Nandakumara K (2005) A Ross score normalization in multimodal biometric systems. Patt Recogn 38:2270–2285
14. Dalal N, Triggs B (2005) Histograms of oriented gradients for human detection. IEEE Comput Soc Conf Comput Vision Patt Recog 1–8
15. Ming-Kuei H (1962) Visual pattern recognition by moment invariants. Informat Theor IRE Trans 8:179–187
16. Silva LF, Saade DCM, Sequeiros-Olivera GO, Silva AC, Paiva AC, Bravo RS, Conci A (2014) A new database for breast research with infrared image. J Med Imag Health Informat 4(1):91–100(9)
17. Tilaki KH (2013) Receiver Operating Characteristic (ROC) curve analysis for medical diagnostic test evaluation. Caspian J Intern Med 4:627–635